Global NEST Journal, Vol 28, No 2, 07737

Spatial network evolution and dynamic convergence pathways of carbon emission efficiency in resource-based cities: A four-stage heterogeneity framework

Wenjing Bao and Haifeng Xiao*
College of Economic & Management, China Agricultural University, Beijing 100083, China
Received: 09/06/2025, Accepted: 23/02/2026, Available online: 27/02/2026
*to whom all correspondence should be addressed: e-mail: haifengxiao@cau.edu.cn
https://doi.org/10.30955/gnj.07737

Graphical abstract

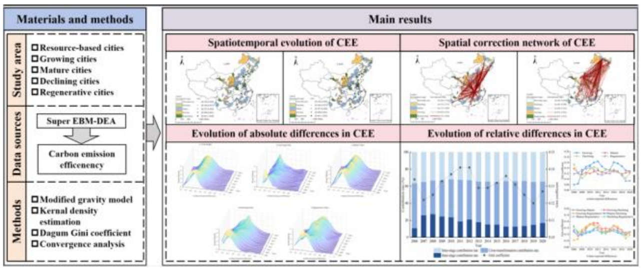

Abstract

Promoting carbon emission efficiency (CEE) development in resource-based cities (RBCs) is critical for achieving China's "carbon peak and carbon neutrality" goals. Current studies frequently cluster these cities without adequately considering their heterogeneity across developmental stages (growing, mature, declining, and regenerative). This study innovatively establishes a four-stage analytical framework, applying the super-EBM DEA model to measure CEE in 110 RBCs (2006-2020) categorized by developmental phase. Integrating a modified gravity model, kernel density estimation, Dagum Gini decomposition, and dynamic convergence analysis, the research reveals: (1) Overall, the level of CEE in RBCs has fluctuated but shown an upward trend, with a distribution pattern that follows "regenerative > growing > mature > declining" cities. (2) The spatial correlation network of CEE of RBCs is characterized by multiple nodes and threads intertwined, which feature spatially proximate correlations and inter-regional connections, with the latter being the dominant mode. (3) Regional differences in CEE among RBCs have generally decreased, although polarization within growing cities remains pronounced. Transvariation density makes the most contribution to the overall Gini coefficient. (4) CEE in RBCs at the overall level exhibits σ convergence, absolute β convergence, and conditional β convergence in space. Each of the four city types shows distinct spatial effects. Factors such as economic development levels, advancements in green technology, and industrial structures have heterogeneous impacts on CEE across RBCs. RBCs should adopt robust carbon emission reduction measures tailored to their unique conditions, facilitating the formation of a reasonably divided, highly efficient, and collaborative framework for reducing carbon emissions.

Keywords: carbon emission efficiency, spatial correlation network, regional differences, spatial convergence, resource-based cities

1. Introduction

Since the Industrial Revolution, anthropogenic greenhouse gas emissions have driven a persistent rise in global surface temperatures, precipitating cascading ecological disruptions, environmental degradation, and socioeconomic challenges (Xiang *et al.* 2025). Controlling carbon emissions has become a global consensus (Gao *et al.* 2017). The international community has responded by establishing multilateral agreements, including the *United Nations Framework Convention on Climate Change*, the *Paris Agreement*, and the *Glasgow Climate Pact*. However, despite concerted governmental efforts across policy, technological, and regulatory dimensions, global carbon emissions continue to rise (Niu *et al.* 2023). The IPCC Sixth Assessment Report underscores this urgency, documenting the increased frequency of extreme heat events across virtually all geographic regions, underlining a clear manifestation of escalating climate risks (Khalid *et al.* 2021). As the world's largest emerging economy and current top carbon emitter, China plays a pivotal role in global climate governance. During the 75th UN General Assembly, China formally announced its "carbon peak and carbon neutrality" targets, which is committing to achieve emission peaking by 2030 and carbon neutrality by 2060. These strategic objectives demonstrate China's proactive engagement in international climate governance and establish a clear roadmap for its domestic decarbonization efforts.

The successful implementation of China's "carbon peak and carbon neutrality" targets hinge on accelerating low-carbon transitions in high-emission regions, particularly resource-based cities (RBCs) that demand immediate decarbonization action (Dong *et al.* 2025). According to the city-level carbon emission statistics from the China Emission Accounts and Datasets (CEADs), approximately one-third of China's carbon emissions originate from RBCs. The per capita carbon emissions in RBCs are 16.1% higher than those in non-resource-based cities, and their energy efficiency is only 62.5% of the latter (Shan *et al.* 2022). These disparities underscore the pressing need to promote the low-carbon transition of RBCs and achieve a virtuous interaction between resource exploitation and urban development. The *National Sustainable Development Plan for Resource-Based Cities* (2013–2020) issued by the State Council of China classifies RBCs into four categories: growing, mature, declining, and regenerative. Due to significant differences among these types in terms of economic foundations, resource endowments, and stages of development, the challenges they face vary considerably, and their progress in emission reduction efforts has also diverged in recent years (Li *et al.* 2019). Existing studies focus on carbon emission intensity, carbon emission efficiency, and their determinants in RBCs (Qiu *et al.* 2017; Liao *et al.* 2022; Guo & Yu 2024; Li *et al.* 2024). However, they typically treat these cities as a unified entity and neglect the heterogeneity across cities with different developmental stages. In view of the research gap, this study focuses on the carbon emission efficiency (CEE) of RBCs at the overall and subtype cities. The results quantify the effectiveness of emission reduction initiatives across RBCs and provide comparative insights into the performance of each type. This research holds important implications for fostering regional cooperation on emission reductions and accelerating the realization of China's "carbon peak and carbon neutrality" targets. Furthermore, it offers empirical support for the low-carbon transformation of RBCs in other developing countries.

The main contributions of this study are as follows: (1) The selection of RBCs as the research object holds strategic significance. Given their dominant role in China's carbon-intensive industries, these cities' decarbonization directly determines the nation's "carbon peak and carbon neutrality" goals realization. Focusing on four specific types (growing, mature, declining, and regenerative) allows capturing transitional heterogeneity, where growing cities face expansion-emission dilemmas while regenerative cities pioneer green innovations, establishing an ideal experimental field for sustainable transition research. (2) This study developed an innovative multidimensional framework for analyzing the evolution of CEE in RBCs. We reveal the static patterns of CEE and decode its dynamic spatial correlation networks by integrating super EBM-DEA with the spatial distribution and using a modified gravity model. Kernel density estimation and Dagum Gini coefficient collaboratively exposed regional differences in CEE. This methodological synthesis overcomes the limitations of single-dimensional analysis in existing literature. (3) Establishing a city-type-oriented convergence model extends conventional convergence theories. The spatial panel regression results verify the differences in convergence among different city types and identify differentiated driving factors, providing empirical evidence for formulating stage-specific decarbonization policy. The findings offer replicable governance paradigms for global resource-based cities.

2. Literature review

2.1. Definition of CEE

CEE refers to the maximum economic growth and minimum carbon emissions achievable without increasing such as capital, labor, and energy inputs. It is a critical metric for evaluating energy conservation and emission reduction efforts (Xiao *et al.* 2023). No official body in China directly publishes data on carbon emissions, necessitating the calculation of these emissions as a first step in studying CEE. Current methodologies for estimating carbon emissions predominantly rely on calculations based on energy consumption. According to the IPCC's guidelines for greenhouse gas emission inventories, multiplying the quantities of fossil fuels consumed by human activities with their respective carbon emission factors and summing these products yields the total carbon emissions for a region or sector (Zheng *et al.* 2023). Only after obtaining this data can one proceed to measure CEE.

Academic research has explored various methods to scientifically assess CEE, evolving from single-factor to multi-factor evaluation approaches. Single-factor evaluations often express CEE as a ratio between total carbon emissions and an economic or energy indicator, such as carbon emission intensity (Wang & Zheng 2021) or carbon productivity (Murshed *et al.* 2022). However, compared to these single-factor metrics, incorporating carbon emissions and energy consumption into a comprehensive total factor productivity growth framework provides a more thorough understanding of the relationship between carbon emissions, all input factors, and economic growth (Yu & Zhang 2021).

2.2. Measurement of CEE

The methods used to measure total-factor CEE include Stochastic Frontier Analysis (SFA) and Data Envelopment Analysis (DEA). SFA is advantageous due to its stochastic nature and allows the estimation of factors influencing CEE (Zhang & Chen 2021). However, a limitation of SFA is that it requires the specification of a particular production function. In contrast, DEA does not have this constraint and can be used to measure efficiencies involving multiple inputs and outputs (Baloch *et al.* 2020). Traditional DEA models include radial CCR/BCC models and non-radial SBM models. The traditional CCR and BCC models overlook non-radial slack variables. Although the SBM model considers these non-radial slacks, it loses the proportion of information between actual and target values of inputs and outputs. The EBM model proposed by Tone and Tsutsui (2010) integrates both radial and non-radial characteristics, preserving the original proportional relationships at the efficiency frontier. However, it cannot differentiate decision-making units with an efficiency score of 1 (Xiao *et al.* 2023). To address these limitations, scholars have made various improvements to DEA models, including the Super SBM, Super EBM, and Super DEA models (Chen 2024; Cui *et al.* 2024; Zheng *et al.* 2024). These advancements have broadened the applicability and effectiveness of DEA in evaluating CEE.

2.3. Research perspectives on CEE

Research on CEE has matured significantly. Studies related to China focus on temporal and spatial evolution (Han *et al.* 2021; Duman *et al.* 2023), spatial characteristics (Shen *et al.* 2021; Lu *et al.* 2023), convergence (Wu *et al.* 2025; Xie *et al.* 2025), and influencing factors (Chen *et al.* 2023; Huang & Yi 2023; Tan *et al.* 2023) of CEE. Early research predominantly focused on provinces as the unit of analysis, but recent literature has shifted toward city-level studies. For instance, Dong *et al.* (2018) examined the temporal changes and driving factors of carbon emission intensity in China, identifying a significant positive impact of industrialization indices on carbon emission intensity. Wang *et al.* (2019) utilized the super EBM model to calculate the CEE of 31 Chinese provinces from 2005 to 2016 and estimated spatial Moran's *I* and LISA clusters. Another study by Wang *et al.* (2020) employed remote sensing data for carbon emissions to construct Markov probability transition matrices and spatial Markov probability transition matrices, investigating the spatiotemporal evolution of urban CEE in China. They found that cities exhibit a club convergence characteristic and suggested cooperation among neighboring cities for energy conservation and emission reduction. As research progresses, the scope has become increasingly detailed, encompassing different industries and specific regions. Su and Xu (2025) analyzed the impact of intelligent manufacturing on CEE using data from 247 manufacturing enterprises in China. Zeng *et al.* (2024) measured the CEE of the transportation industry along China's Yangtze River Economic Belt from 2014 to 2020, finding that economic development levels and population density significantly influence CEE. Xue *et al.* (2022) assessed CEE in the Beijing-Tianjin-Hebei region and used spatial quantile models to estimate influencing factors. Lastly, Xing *et al.* (2024) applied the SBM-DDF model to measure CEE across 284 Chinese cities and used machine learning algorithms to identify city-specific characteristics.

Research focusing specifically on RBCs remains relatively sparse within the broader field of CEE. Qiu *et al.* (2017) analyzed the relationship between carbon emissions and industrial structure transformation using decoupling indices in the context of the Xuzhou Metropolitan Area. Liao *et al.* (2022) measured the carbon emission intensity of RBCs in China in 2012, identifying industrial energy carbon emissions as the primary source for these cities. Li *et al.* (2024) utilized the LMDI method to explore the contributions of different city types, industries, and driving factors to carbon emissions across 83 RBCs from 2005 to 2017. Song *et al.* (2022) examined carbon emission intensity in RBCs from a developmental stage perspective, analyzing spatiotemporal evolution characteristics and the heterogeneity of influencing factors. Guo and Yu (2024) applied spatial data analysis and geographically weighted regression methods to investigate the spatial patterns and influencing factors of 113 RBCs in China.

Despite these contributions, several limitations persist in the research on CEE specific to RBCs: (1) There is a scarcity of quantitative studies focusing on the CEE of RBCs. Existing quantitative analyses often focus on provinces or single cities, or they analyze only a single year, which fails to capture the trends in CEE changes over recent years for RBCs. (2) Most studies on RBCs have concentrated on the temporal and spatial evolution of CEE and its influencing factors. However, there is a relative lack of quantitative analysis on the spatial correlation networks, regional disparities, and convergence of CEE in RBCs at the overall and subtype level. This gap limits our ability to identify dynamic evolutionary paths and internal heterogeneities in CEE among RBCs.

Table 1. Classification list of RBCs.

Type	City list	Count
Growing	Shuozhou, Hulunbuir, Ordos, Songyuan, Hezhou, Nanchong, Liupanshui, Zhaotong, Yan'an , Xianyang, Yulin, Wuwei, Qingyang, and Longnan	14
Mature	Zhangjiakou, Chengde, Xingtai, Handan, Datong, Changzhi, Jincheng, Xinzhou, Jinzhong, Linfen, Yuncheng, Lüliang, Chifeng, Benxi, Jilin, Heihe, Daqing, Jixi, Mudanjiang, Huzhou, Suzhou, Bozhou, Huainan, Chuzhou, Chizhou, Xuancheng, Nanping, Sanming, Longyan, Ganzhou, Yichun, Dongying, Jining, Tai'an, Sanmenxia, Hebi, Pingdingshan, Ezhou, Hengyang, Chenzhou, Shaoyang, Loudi, Yunfu, Baise, Hechi, Guangyuan, Zigong, Panzhihua, Dazhou, Ya'an, Anshun, Qujing, Baoshan, Lincang, Weinan, Baoji, Jinchang, and Pingliang	58
Declining	Wuhai, Fuxin, Fushun, Liaoyuan, Baishan, Yichun, Hegang, Shuangyashan, Qitaihe, Huaibei, Tongling, Jingdezhen, Xinyu, Pingxiang, Zaozhuang, Jiaozuo, Puyang, Huangshi, Shaoguan, Luzhou, Tongchuan, Baiyin, and Shizuishan	23
Regenerative	Tangshan, Baotou, Anshan, Panjin, Huludao, Tonghua, Xuzhou, Suqian, Ma'anshan, Zibo, Linyi, Luoyang, Nanyang, Lijiang, and Zhangye	15

3. Methodology and data

3.1. Study area

According to the *National Sustainable Development Plan for RBCs* (2013-2020) (referred to as the Plan), RBCs are those where the dominant industries involve the extraction and processing of local natural resources such as minerals and forests. These include prefectural-level divisions (such as prefecture-level cities, regions, autonomous prefectures, leagues, etc.), county-level cities, counties (including autonomous counties, forest regions, etc.), and districts of cities (development zones, management zones). China has 262 RBCs, comprising 126 prefectural-level divisions, 62 county-level cities, 58 counties, and 16 city districts. Considering data availability and comparability, this study selected 110 prefecture-level cities out of the 126 prefectural-level divisions as the basic research units, with the research period spanning from 2006 to 2020. Given that resource exploitation in RBCs is at different stages, the Plan categorizes these cities into four types: growing, mature, declining, and regenerative. The distribution of the sample among these types is detailed in **Table 1**.

3.2. Methodology

3.2.1. Super EBM-DEA model

Total-factor CEE has been widely used to assess the relationship between environmental protection and economic growth, promote low-carbon economic development, and ensure the sustainability of economic growth. Therefore, this study measured the CEE of RBCs under a total-factor productivity framework. According to research by Färe *et al.* (2007), this study used energy consumption, labor, and capital as input indicators, treating the GDP of cities as desirable outputs while considering urban carbon emissions as undesirable outputs (see **Table 2** for details).

Table 2. Input and output index system of CEE.

Primary indicator	Secondary indicator	Tertiary indicator
Input indicators	Labor	Measured by the number of employed persons (ten thousand) in each prefecture-level city over the years.
	Capital	Capital stock was calculated using the perpetual inventory method with 2006 as the base year, following the approaches of Goldsmith (1951) and Gao *et al.* (2021). The specific formula as follows. $K_{i,t}=K_{i,t-1}(1-\delta_{i,t})+I_{i,t}$, where $K_{i,t}$ is capital stock of city *i* in year *t* (RMB 100 million); $\delta_{i,t}$ is depreciation rate, set at 9.6% following Hou *et al.* (2024) ; $I_{i,t}$ is capital investment (RMB 100 million).
	Energy	Urban direct energy consumption mainly includes natural gas and liquefied petroleum gas, while indirect energy consumption is primarily electricity usage. Due to the unit's inconsistency, energy consumption was converted into standard coal equivalents. According to the "General Principles for Calculation of Comprehensive Energy Consumption," the conversion coefficients are 1.3300 kgce/m³ for natural gas, 1.7143 kg/kg for liquefied petroleum gas, and 0.1229 kg/(kW·h) for electricity.
Desirable outputs	City GDP	Gross Domestic Product (GDP) of each city, calculated at constant 2006 prices (RMB 10,000 yuan), reflecting economic output as a desirable outcome.
Undesirable outputs	City carbon emissions	Carbon emissions include direct emissions from fossil fuels such as natural gas and liquefied petroleum gas and indirect emissions from electricity and heat consumption. The calculation method follows Zheng *et al.* (2023), which aligns with IPCC guidelines for greenhouse gas accounting, incorporating emission factors for different energy sources.

The EBM model proposed by Tone and Tsutsui (2010) cannot differentiate between decision-making units (DMUs) with an efficiency score of 1. To address this limitation and further evaluate efficient DMUs, this study adopted the approach by Andersen and Petersen (1993). Each city is treated as a DMU to construct the best-practice frontier for CEE across different cities. Assuming there are *n* DMUs (*j*=1, ..., *n*) at time *t* (*t*=1, ..., *T*), each DMU has *m* types of input factors x_{ij} (*i*=1, ..., *m*), *s* desirable outputs y_{rj} (*r*=1, ..., *s*), and *h* undesirable outputs b_{zj} (*z*=1, ..., *h*). The study employed a window DEA model with a moving average technique to calculate panel data. This method treats DMUs from different periods as distinct entities, allowing for efficiency measurement over time. Drawing on the research by Charnes *et al.* (1995), this study set the window width to 4 years, resulting in 15 windows. The super EBM-DEA model addresses the limitations of the traditional EBM model and optimizes the calculation results for CEE. Below is the detailed formulation of the model:

$$\gamma^*=\min\frac{\theta-\varepsilon_x\sum_{i=1}^{m}\frac{w_i^- s_i^-}{x_{io}}}{\varphi+\varepsilon_y\sum_{r=1}^{s}\frac{w_r^+ s_r^+}{y_{ro}}+\varepsilon_b\sum_{z=1}^{h}\frac{w_z^- s_z^-}{b_{zo}}} \tag{1}$$

$$s.t.\begin{cases}\sum_{t=1}^{T}\sum_{j=1,j\neq o}^{n}\lambda_j x_{ij}+s_i^-=\theta x_{io}, i=1,\dots,m\\ \sum_{t=1}^{T}\sum_{j=1,j\neq o}^{n}\lambda_j y_{rj}-s_r^+=\varphi y_{ro}, r=1,\dots,s\\ \sum_{t=1}^{T}\sum_{j=1,j\neq o}^{n}\lambda_j b_{zj}+s_z^-=\varphi b_{zo}, z=1,\dots,h\\ \lambda_j\geq 0, s_i^-\geq 0, s_r^+\geq 0, s_z^-\geq 0\end{cases}$$

where, γ^* represents the optimal efficiency of the composite decision-making unit; ; x_{io} , y_{ro} , and b_{zo} denote the input resources, desirable outputs, and undesirable outputs of the evaluated unit *o*, respectively; s_i^- , s_r^+ , and s_z^- are the slack variables corresponding to inputs, desirable outputs, and undesirable outputs, respectively; w_i^- , w_r^+ , and w_z^- are the weights assigned to inputs, desirable outputs, and undesirable outputs, all of which are greater than or equal to 0 ; ε_x , ε_y , and ε_b represent the non-radial weights for inputs, desirable outputs, and undesirable outputs, respectively; θ and φ are the radial efficiency score and the output expansion factor, subject to the constraints $0<\theta\leq 1$ and $\varphi>1$; λ_j is the linear combination coefficient.

3.2.2. Modified gravity model

Numerous studies have demonstrated the spatially dependent nature of regional carbon emissions. Leveraging the positive externalities associated with economic or urban agglomeration may effectively counteract the environmental degradation caused by such emissions (Shen *et al.* 2021). The Vector Autoregression (VAR) model and the gravity model are the primary methods used to examine spatial association relationships (Gao and Gao 2024). However, the VAR model has limitations. It cannot reveal the dynamic characteristics of spatial association networks and is highly sensitive to the choice of lag order (Balsalobre-Lorente *et al.* 2019). To address these issues, this study adopted a modified gravity model inspired by Li *et al.* (2024) to integrate CEE with geographical distance, effectively reflecting the dynamics of spatial associations.

Based on the gravitational values of CEE from 110 RBCs, an initial spatial association matrix (110×110) is constructed. The average value of each row in the matrix is used as a threshold. Gravitational values above this threshold are retained, indicating a spatial correlation between city *i* and city *j*. Values below the threshold are set to 0, implying no spatial correlation between the cities. After this processing step, a final spatial association matrix for CEE of RBCs is obtained. The calculation formula for this process is as follows:

$$F_{ij}=k_{ij}\frac{CEE_i\times CEE_j}{D_{ij}^2},k_{ij}=\frac{CEE_i}{CEE_i+CEE_j} \tag{2}$$

where, F_{ij} is the gravitational values, represents the overall spatial association intensity of CEE; k_{ij} is the modified gravitational index indicating city *i*'s contribution coefficient to the spatial association intensity of CEE between city *i* and city *j*; D_{ij}^2 is the geographical distance (m) between cities *i* and *j*; CEE_i and CEE_j represent CEE of city *i* and *j*.

3.2.3. Kernal density estimation

Kernel density estimation is a non-parametric method commonly used to characterize the distribution features of CEE (Heidenreich *et al.* 2013). Kernel density estimation generates continuous probability density curves by applying smoothing techniques to observed data, which helps identify key characteristics of the distribution and provides an intuitive visualization of the overall data pattern. The main advantage of Kernel density estimation lies in its data-driven nature, which avoids subjective biases arising from assumptions about functional forms in parametric estimation and allows for a more accurate reflection of the underlying data distribution. The center of the curve reflects the central tendency, indicating the overall level of CEE. The shape of the curve reveals the distribution's symmetry or skewness. The width of the curve indicates the dispersion or spread of CEE values—when the tails are elongated, it suggests increasing disparities among samples. The number of peaks reflects the dominant groups within the distribution—an evolution from unimodal to bimodal suggests a polarization trend among the samples. The formula of the kernel density estimator is as follows:

$$f(x)=\frac{1}{Nh}\sum_{i=1}^{N}K\left(\frac{X_i-x}{h}\right) \tag{3}$$

where, *N* denotes the number of observations; *h* is the bandwidth, which controls the degree of smoothing; *x* represents the variable of interest; X_i are the observed values. *K*(·) is the Kernel function. The widely used Gaussian Kernel function was employed in this study to calculate the Kernel density values. Its mathematical expression is as follows:

$$K(x)=\frac{1}{\sqrt{2\pi}}\exp(-\frac{x^2}{2}) \tag{4}$$

3.2.4. Dagum Gini coefficient

In regional differences studies, scholars often utilize three methods: the Theil index, the traditional Gini coefficient, and the Dagum Gini coefficient. Among these, the Theil index and the traditional Gini coefficient present challenges when analyzing regional differences in CEE. These methods require data to conform to specific statistical assumptions, such as normal distribution and homoscedasticity, and they are not adept at handling overlapping situations between different regions. To address these issues, this study adopted the Dagum Gini coefficient. This method can more accurately analyze regional disparities and the underlying causes of CEE in China's RBCs. The formula is as follows:

$$G=\frac{\sum_{h=1}^{k}\sum_{r=1}^{k}\sum_{i=1}^{n_j}\sum_{j=1}^{n_h}\left|CEE_{hi}-CEE_{rj}\right|}{2n^2\overline{CEE}},G=G_w+G_{nb}+G_t \tag{5}$$

where, *G* represents the overall Gini coefficient of CEE among RBCs; *h* and *r* denote study areas (the four subtype cities); *i and j* refer to cities within these study areas; k is the number of RBCs types, k=4; n represents the number of cities within a specific study area; CEE_{hi} and CEE_{rj} indicate the CEE of the city *i* in area *h* and city *j* in area *r*, respectively; $\overline{CEE}$ denotes the mean CEE of RBCs. Furthermore, the overall Gini coefficient of CEE can be decomposed into three parts: intra-regional differences G_w, inter-regional differences G_{nb}, and transvariation density G_t. For detailed calculation methods, refer to Dagum's research (Dagum 1997).

3.2.5. Convergence analysis

The study of convergence issues originally stems from neoclassical growth theory (Solow 1988). This theory posits that assuming identical technological conditions, the economic growth rate of less developed countries will be faster than that of developed countries due to diminishing marginal returns on capital. Consequently, less developed countries will gradually approach the economic levels of developed countries, reaching a steady state. As convergence models have been widely applied in economics, their use has expanded beyond studying economic growth to analyzing other issues, such as the efficiency of technology resource allocation (Bai & Lin 2024) and changes in carbon productivity (Shen *et al.* 2021). In China, the progress towards achieving “carbon peak and carbon neutrality” may lead to stabilization in CEE over time. Therefore, it is highly appropriate to use convergence models to study the long-term trends in CEE among China’s RBCs.

Convergence models include *σ* convergence, *β* convergence, and so on. *σ* convergence refers to the trend where deviations in CEE among cities decrease over time. This type of convergence can be measured using the coefficient of variation. The calculation formula is as follows:

$$\sigma=\frac{\sqrt{\sum_{i=1}^{N_j}(CEE_{ij}-\overline{CEE_{ij}})^2/N_j}}{\overline{CEE_{ij}}} \tag{6}$$

where, *CEE*$_{ij}$ represents the CEE of city *j* within region i; $\overline{CEE_{ij}}$ denotes the mean CEE within region j; *N*$_j$ indicates the number of cities within region j.

β convergence refers to the process in which regions with lower CEE gradually catch up with those having higher efficiency over time, leading to a narrowing gap and eventual convergence toward the same level. Depending on whether includes external influencing factors, *β* convergence can be classified into absolute *β* convergence and conditional *β* convergence. Considering that CEE can show spatial relationships between regions, it is essential to include spatial interactions when examining convergence mechanisms. Commonly used spatial econometric models include the Spatial Autoregressive Model (SAR), the Spatial Error Model (SEM), and the Spatial Durbin Model (SDM). The spatial absolute *β* convergence model extends the traditional absolute *β* convergence framework by incorporating spatial interactions, allowing a more accurate analysis of the catching-up effect between regions. The model is specified as follows:

$$\text{SAR:}\ln\left(\frac{CEE_{i,t+1}}{CEE_{i,t}}\right)=\alpha+\beta\ln(CEE_{i,t})+\rho\sum_{j=1}^{n}w_{ij}\ln\left(\frac{CEE_{i,t+1}}{CEE_{i,t}}\right)+\mu_i+\eta_t+\varepsilon_{i,t} \tag{7}$$

$$\text{SEM:}\ln\left(\frac{CEE_{i,t+1}}{CEE_{i,t}}\right)=\alpha+\beta\ln(CEE_{i,t})+\mu_i+\eta_t+u_{i,t},u_{i,t}=\lambda\sum_{j=1}^{n}w_{ij}u_{i,t}+\varepsilon_{i,t} \tag{8}$$

$$\text{SDM:}\ln\left(\frac{CEE_{i,t+1}}{CEE_{i,t}}\right)=\alpha+\beta\ln(CEE_{i,t})+\rho\sum_{j=1}^{n}w_{ij}\ln\left(\frac{CEE_{i,t+1}}{CEE_{i,t}}\right)+\gamma\sum_{j=1}^{n}w_{ij}\ln(CEE_{i,t})+\mu_i+\eta_t+\varepsilon_{i,t} \tag{9}$$

where, $CEE_{i,t+1}$ is the CEE of city *i* in period *t*+1; $CEE_{i,t}$ is the CEE of city *i* in period *t*; $\ln\left(CEE_{i,t+1}/CEE_{i,t}\right)$ represents the CEE growth rate for city *i* in period *t*+1; *α* is a constant; *β* is the convergence coefficient. If *β*<0, it indicates a convergence effect in CEE; otherwise, a divergence trend exists. *v* represents the convergence speed, $v=-\ln(1-|\beta|)/T$; *ρ* is the spatial lag coefficient, indicating the impact of neighboring cities’ CEE growth rates; *λ* is the spatial error coefficient, reflecting spatial effects present in the random disturbance term; *γ* is the spatial lag coefficient of the independent variables, representing the influence of neighboring cities’ CEE; w_{ij} denotes the spatial weight. To avoid endogeneity caused by socio-economic distance, the spatial weight matrix was constructed using the inverse of the squared geographic distance between cities — that is, as geographical distance increases, the correlation of CEE between cities gradually weakens (Qu & Lee 2015). μ_i , η_t and $\varepsilon_{i,t}$ represent regional effects, time effects, and the random disturbance term, respectively.

Conditional *β* convergence extends the concept of absolute *β* convergence by incorporating control variables to examine whether regional CEE exhibits a convergence trend when controlling for exogenous influencing factors. The spatial conditional *β* convergence model is specified as follows:

$$\text{SAR:}\ln\left(\frac{CEE_{i,t+1}}{CEE_{i,t}}\right)=\alpha+\beta\ln(CEE_{i,t})+\rho\sum_{j=1}^{n}w_{ij}\ln\left(\frac{CEE_{i,t+1}}{CEE_{i,t}}\right)+\delta X_{i,t+1}+\mu_i+\eta_t+\varepsilon_{i,t} \tag{10}$$

$$\text{SEM:}\ln\left(\frac{CEE_{i,t+1}}{CEE_{i,t}}\right)=\alpha+\beta\ln(CEE_{i,t})+\delta X_{i,t+1}+\mu_i+\eta_t+u_{i,t},u_{i,t}=\lambda\sum_{j=1}^{n}w_{ij}u_{i,t}+\varepsilon_{i,t} \tag{11}$$

$$\text{SEM:}\ln\left(\frac{CEE_{i,t+1}}{CEE_{i,t}}\right)=\alpha+\beta\ln(CEE_{i,t})+\delta X_{i,t+1}+\mu_i+\eta_t+u_{i,t},u_{i,t}=\lambda\sum_{j=1}^{n}w_{ij}u_{i,t}+\varepsilon_{i,t} \tag{12}$$

where, $X_{i,t+1}$ represents a series of control variables affecting CEE in RBCs, and *δ* denotes the vector of parameters. Drawing on the studies by Xu *et al.* (2023), Jiang *et al.* (2024), and Liu *et al.* (2025), the following control variables were selected. Economic development level (GDP): Measured by the regional gross domestic product (billion yuan). Economic development level squared (GDP^2): The square of the regional GDP (billion yuan squared). Green technology progress (GTP): Measured by the number of green patents granted in a year (thousands). Population density (POP): Calculated as the ratio of the registered population at the end of the year to the administrative area's land size. Environmental regulation (ER): Measured by the proportion of fiscal expenditure on energy conservation and environmental protection relative to GDP. Industrial structure advancement (ISA): Calculated as the ratio of the added value of the tertiary industry to that of the secondary industry. Industrial structure rationalization (ISR): Measured using the Theil index. Descriptive statistics for CEE and control variables are presented in **Table 3**.

Table 3. Descriptive statistics of variables.

Variable	Observation	Mean	S.D.	Mix	Max
CEE	1650	0.513	0.131	0.193	1.046
GDP	1650	1208.353	1075.096	70.175	7320
GDP^2	1650	2645248	5440871	7194.093	53582400
GIP	1650	0.009	0.017	0	0.186
POP	1650	320.858	252.338	9.653	1483.707
ER	1650	0.033	0.019	0.005	0.193
ISA	1650	0.847	0.441	0.131	3.759
ISR	1650	0.229	0.081	0.039	0.415

Note: The economic development level, the economic development level squared, and green technology progress were logged in regression analysis. The formula for calculating the Theil index is as follows: $TL = \sum_{i=1}^{n}(Y_i / Y)\ln[(Y_i / Y)/(Y/L)]$ *, where* Y *represents GDP (billion yuan),* L *represents the number of employees in the industry (ten thousand people),* i*=1, 2, 3 denote the primary, secondary, and tertiary industries, respectively;* n *is the number of industries (units).*

3.3. Data resources

This study used 110 resource-based prefectural-level cities from 2006 to 2020 as the basic research units. Data on CEE calculations and control variables were primarily sourced from the *China City Statistical Yearbook* and the *China Urban Construction Statistical Yearbook* from 2007 to 2021. The study measured the geographic distances between cities by calculating spherical distances using the point distance tool in ArcGIS software. Basic geographic information data were from the Standard Map Service website of the China Ministry of Natural Resources (http://bzdt.ch.mnr.gov.cn). Green patent data were from the China National Intellectual Property Administration. For the few missing data points, we used a linear interpolation supplement.

4. Results and discussion

4.1. Characterization of spatiotemporal evolution

From 2006 to 2020, CEE in China's RBCs increased significantly, with an average annual growth rate of 2.18%, indicating that China has made progress in reducing carbon emissions. The study period can be divided into two phases (**Figure 1**). The first phase, from 2006 to 2012, is a period of rapid growth. During this time, the average CEE rose from 0.413 to 0.558, with an annual growth rate as high as 5.4%. This stage coincided with the implementation period of China's energy conservation and emission reduction work during the 11th Five-Year Plan. During the "11th Five-Year Plan" period, China supported an average annual growth rate of 11.2% in the national economy, with an average annual growth rate of 6.6% in energy consumption. The energy consumption elasticity coefficient decreased from 1.04 during the "10th Five-Year Plan" period to 0.59, resulting in a savings of 630 million tons of standard coal. The capacity for sustainable development has improved, and the efficiency of carbon emissions has increased gradually.

The second phase, from 2013 to 2020, is characterized by slow and fluctuating growth. In 2013, the average CEE slightly declined to 0.533, followed by a gradual increase to 0.554 by 2020. In November 2013, the Chinese government released the "*National Sustainable Development Plan for Resource-based Cities (2013-2020)*". This was the first time that the Chinese government had developed a comprehensive and detailed plan for the sustainable development of RBCs, representing a significant milestone in their development (Ruan *et al.* 2020). The plan has prompted governments at all levels to consider the sustainable development of RBCs. The necessity to transform the prevailing economic growth model from an extensive expansion to an intensive and efficient development model is emphasized. At the national level, it has strengthened the development concept of classified guidance for different types of RBCs, emphasizing the cultivation of new economic growth poles based on local conditions. Based on this document, in 2017, the "*Guiding Opinions on Strengthening Classified Guidance to Cultivate New Driving Forces for the Transformation and Development of Resource-based Cities*" was issued, clearly defining the different goals for the four types of RBCs.

The CEE of the four subtypes of RBCs all exhibit a fluctuating growth trend. Overall, the distribution pattern can be described as "regenerative > growing > mature > declining." From 2006 to 2020, the average carbon emission efficiencies for regenerative, growing, mature, and declining cities were 0.548, 0.543, 0.508, and 0.484, respectively, indicating notable differences among these city types. Regenerative cities have been in the lead since 2016, with an average annual growth rate of 2.89% in CEE. The optimization of industrial structures and innovation-driven strategies in these regions effectively support efficient emission reductions. Growing cities experienced rapid growth in CEE before 2012, reaching a peak in 2016, followed by a fluctuating decline, highlighting the diminishing marginal benefits of environmental governance during periods of resource expansion. Mature cities saw a moderate increase in CEE at an average annual growth rate of 1.67%, although traditional industrial models and path dependence constrain their transformation processes. Despite having the lowest average CEE, declining cities began to show an upward trend after 2015, surpassing growing cities by 2020. For these regions, investments in clean technologies driven by resource depletion become a critical force for transformation.

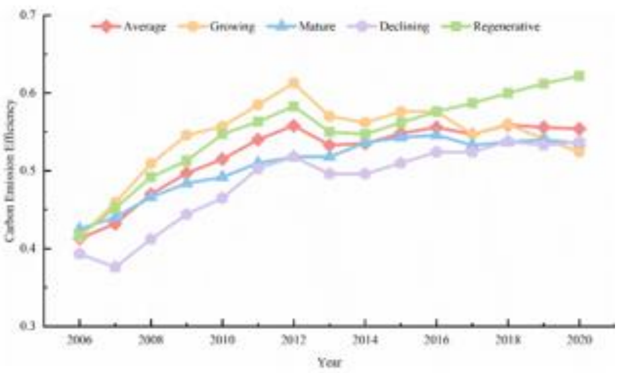

Figure 1. CEE of RBC from 2006 to 2020.

This study adopted an equal-interval classification method to visually examine the spatial distribution characteristics of CEE in RBCs. The CEE values of RBCs in 2006 and 2020 were divided into five categories: low-level ($0.193 \leq$ CEE<0.360), lower-middle level ($0.360 \leq$ CEE < 0.527), middle-level ($0.527 \leq$ CEE<0.694), upper-middle level ($0.694 \leq$ CEE<0.861), and high level ($0.861 \leq$ CEE$\leq$1.028). As shown in **Figure 2**, there are differences in CEE among RBCs. In 2006, most RBCs fell into the lower-middle level category (63 cities), of which 54.0% were mature cities, 17.4% were growing cities, and both declining and regenerative cities accounted for 14.3%. There were 35 cities in the low-level group, with 48.6% located in mature cities and 34.3% in declining cities; growing and regenerative cities made up a smaller proportion. 10 cities belonged to the middle level, mainly distributed across mature cities. Only 1 city each was classified as upper-middle level (Fuxin) and high level (Ezhou), respectively.

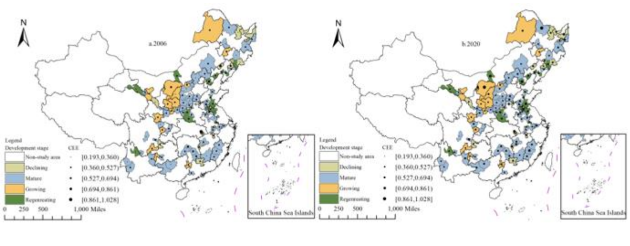

Figure 2. Evolution of the spatial pattern of CEE of RBCs in 2006 and 2020.

By 2020, a pattern of "three increases and two decreases" emerged compared to 2006. The number of cities in the middle, upper-middle, and high-level categories increased, while those in the low and lower-middle levels decreased. The dominant category shifted from the lower-middle level to the middle level. The number of high-level cities grew to 2: Heihe and Ordos. The number of upper-middle level cities rose to 10, primarily concentrated in mature and regenerative cities. Middle-level cities increased to 48, mainly found in declining and mature cities. Lower-middle level cities decreased to 46, with mature cities still accounting for the largest share (54.3%). Finally, only 4 cities remained in the low-level category: Datong, Tongchuan, Dazhou, and Ya'an.

4.2. Characterization of spatial correction network

This study utilized ArcGIS software to map the spatial correlation networks of CEE in China's RBCs for 2006 and 2020 (**Figure 3**). The research revealed that the spatial correlation strength of CEE increased from 0.086 to 0.149, a rise of 73.3%, indicating a gradual enhancement of synergistic effects among RBCs. The total number of correlations grew from 5,883 to 6,224, an increase of 5.8%. Although spatial correlation has strengthened, it remains significantly below the theoretical maximum of 11,990 connections (110 × 109), with a potential connection gap of 46.3%. The spatial correlation network of CEE exhibits complex characteristics, specifically manifested as multiple nodes and threads interwoven alongside the coexistence of spatially proximate and inter-regional associations. In 2006, the network exhibited a web-like structure centered around 5 mid-western cities, including Ezhou and Zigong. Among these core cities, mature and declining cities accounted for a ratio of 3:2, forming a single-core radiation model centered on traditional industrial bases. By 2020, this structure had evolved into a more dispersed network with nodes encompassing various city types, such as Heihe and Wuhai. Taking advantage of its location along the China-Russia border, Heihe City has developed a thriving port economy and cross-border cooperation. In recent years, the city has increased investment promotion, accelerated the development of the ecological industry, promoted green development, and established a government-market-urban-rural co-driven model. Wuhai City, as a core coal and coke base in China, is also undergoing industrial transformation and upgrading by actively developing a green circular economy. The city has shifted its production mode from loose to processing type and has become a pilot city for green transformation and a demonstration city for circular economy in RBCs nationwide (Gong 2024).

Focusing on the top 500 city pairs with high gravitational values, this study found that inter-regional spatial associations dominate the CEE of RBCs. There were 323 inter-regional spatial association pairs in 2006, with mature-declining city pairs accounting for the largest share at 22.6%. There were also 177 intra-regional spatial association pairs, with mature-mature city pairs making up the largest share at 30.0%. By 2020, the number of inter-regional spatial association pairs had increased to 359, with mature-regenerative city pairs (24.6%) becoming the most prevalent combination. The number of intra-regional spatial association pairs decreased to 141, with mature-mature city pairs (17.5%) still being the most common combination. This structural shift aligns closely with the timing of China's post-2013 pilot policies aimed at transforming RBCs.

Notably, the internal connections between regenerative cities have strengthened, with the number of regenerative-regenerative city pairs increasing from 1.6%

in 2006 to 6.6% in 2020, representing a rise of 312.5%. The findings indicate that successfully transformed regenerative cities have formed a low-carbon technology spillover effect. Regarding declining cities, there has been a substantial increase in the strength of their associations with regenerative cities. Despite this, the internal associations among declining cities continue to be weak. This phenomenon suggests that declining cities fell into a path dependency trap during their development and transformation processes.

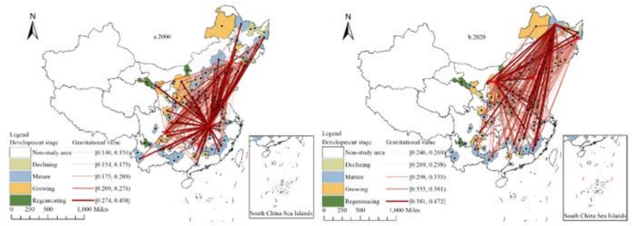

Figure 3. Spatial correlation network of CEE of RBCs in 2006 and 2020.

4.3. Analysis of Regional difference in CEE

To further analyze the regional differences of CEE in RBCs, this study first employed Kernel density estimation to explore the evolution of absolute differences in CEE from four aspects: distribution location, distribution shape, distribution extensibility, and peak characteristics (**Figure 4**). Secondly, the Dagum Gini coefficient of CEE in RBCs was calculated and decomposed to clarify the trajectory of relative differences and identify the primary sources of regional differences in CEE among RBCs (**Figures 5 and 6**).

4.3.1. Analysis of the evolution of absolute difference

In the 3D Kernel density plot, the vertical axis represents Kernel density values, the horizontal axis represents CEE, and the lateral axis represents the study period. From an overall perspective of RBCs, the Kernel density curves of CEE exhibited a positively skewed distribution with a right tail. The center of the curve had shifted to the right, and the height of the main peak shows a fluctuating downward trend. This evaluation indicates that the CEE of RBCs has generally improved over time; however, there were significant disparities in the pace of improvement across cities. A few cities had substantial progress, while the major cities remain at medium-to-low efficiency levels. Meanwhile, the increasing dispersion in efficiency distribution indicated a progressive reduction in regional absolute difference.

When comparing the four types of RBCs, the findings are as follows:(1) The distribution centers of the Kernel density curve for each type of RBCs showed varying degrees of rightward shift, consistent with the overall trend. It indicated that the CEE of each type of resource-based city is continuously improving. (2) The heights of the main peaks of the Kernel density curves for each type exhibited a fluctuating downward trend, suggesting that the absolute differences in CEE within each type of city are decreasing. (3) All four types of RBCs exhibited a right-tail phenomenon. Specifically, the Kernel density curves of mature, declining, and regenerative cities converged towards the right annually, indicating that the gap between extreme values and average values of CEE within these three types of cities is narrowing over time. In contrast, the convergence of the Kernel density curve for growing cities was less pronounced, highlighting that the gap between extreme values and average values within growing cities remains significant. (4) Only growing cities exhibited a “one main peak with multiple side peaks” phenomenon, indicating a trend of two or more polarizations in CEE within growing cities. The significant difference in peak heights and distances between the main and side peaks highlighted notable spatial polarization. In contrast, the other three types of RBCs displayed single peaks and did not exhibit spatial polarization trends.

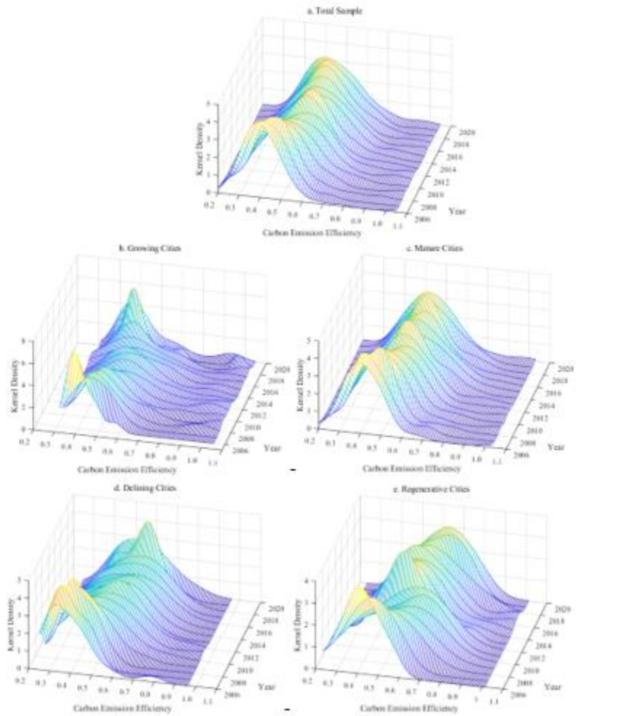

Figure 4. Evolution of absolute differences in CEE of RBCs.

4.3.2. Analysis of the evolution of relative difference

Overall, the Dagum Gini coefficient of CEE for RBCs showed a fluctuating downward trend, decreasing from 0.134 in 2006 to 0.127 in 2020. It indicated a gradual narrowing of regional differences over time, with a total decline of 5.22%. The contribution of transvariation density remains the highest, with an average share of 47.98%, making it the primary source of relative differences in CEE among RBCs. The intra-regional contribution is 33.99%, while the inter-regional contribution is 18.04%. The significant contribution of transvariation density suggested that a relatively high proportion of outlier cities exist—those that deviated from their group and moved into higher or lower efficiency categories. Taking 2006 as an example, the average CEE of regenerative cities was 0.417, which was at a relatively high level that year; however, Lijiang within this group had a much lower efficiency value of 0.235, far below the group average. Similarly, the average efficiency of declining cities was 0.393, placing them at a relatively low level overall, yet Fuxin within this group exhibited a significantly higher efficiency of 0.785. This phenomenon persisted in 2020. For instance, Heihe broke away from other mature cities and entered the high-efficiency category with an efficiency score of 0.984. Likewise, most regenerative cities performed above the average efficiency of RBCs, but Zhangye within this group had a relatively low efficiency of 0.457.

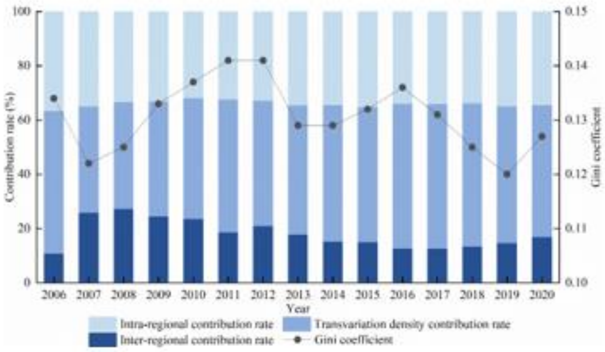

Figure 5. Decomposition of CEE differences in RBC from 2006 to 2020.

The differences in CEE within and between the four types of RBCs exhibited a convergence trend, as illustrated in **Figure 6**. From the perspective of intra-regional differences, the Gini coefficients for mature, declining, and regenerative cities all showed varying degrees of decline: regenerative cities (21.01%) > declining cities (20.92%) > mature cities (7.97%), which aligns with the Kernel density analysis results. In contrast, the Gini coefficient for growing cities displayed an "M"-shaped fluctuating growth trend, increasing by 61.25% from 2006 to 2020. Although the absolute differences among growing cities have slightly decreased, the relative differences have significantly increased. It is due to an increase in cities with higher CEE in 2020, as indicated by the Kernel density analysis.

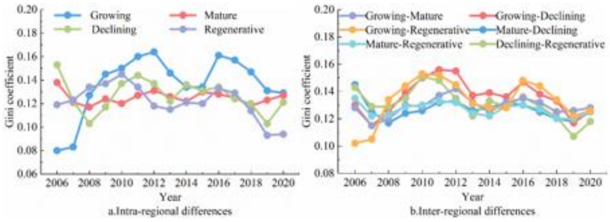

Figure 6. Gini coefficient of CEE in RBCs from 2006 to 2020.

Regarding inter-regional differences, the Gini coefficients between the four types of RBCs followed an "M"-shaped variation trend. Specifically, the Gini coefficient between growing and regenerative cities showed a fluctuating upward trend, increasing by 23.99%. The Gini coefficient between mature and growing cities was close at the beginning and end of the study period. For other inter-regional comparisons, the Gini coefficients exhibited a fluctuating downward trend. Notably, the relative difference between declining and regenerative cities had decreased the most (17.54%), while the difference between declining and growing cities had declined the least (2.94%).

Table 4. The σ convergence coefficient of CEE in RBCs from 2006 to 2020.

Year	Overall	Growing	Mature	Declining	Regenerative
2006	0.530	0.157	0.285	0.305	0.219
2007	0.533	0.151	0.224	0.202	0.225
2008	0.521	0.284	0.221	0.188	0.245
2009	0.512	0.314	0.244	0.217	0.249
2010	0.503	0.314	0.217	0.253	0.264
2011	0.495	0.317	0.240	0.281	0.247
2012	0.488	0.327	0.244	0.252	0.215
2013	0.507	0.282	0.231	0.220	0.219
2014	0.520	0.257	0.220	0.244	0.228
2015	0.516	0.258	0.232	0.235	0.228
2016	0.511	0.312	0.231	0.239	0.267
2017	0.505	0.306	0.227	0.221	0.256
2018	0.499	0.303	0.216	0.215	0.209
2019	0.504	0.283	0.220	0.188	0.168
2020	0.501	0.275	0.237	0.219	0.170

4.4. Convergence analysis of CEE

4.4.1. σ convergence analysis

Table 4 shows the σ convergence results of CEE for RBCs at the overall and four subtypes level from 2006 to 2020. Overall, the coefficient of variation (CV) for CEE in RBCs exhibited a fluctuating downward trend, decreasing from 0.530 in 2006 to 0.501 in 2020, a reduction of 5.47%. It indicated that RBCs exhibit significant σ convergence characteristics in CEE. Among the four types of RBCs, declining, regenerative, and mature cities all showed σ convergence. Specifically, declining cities had intensive convergence, with their CV decreasing by 28.39%. Regenerative cities followed with a CV reduction of 22.22%, while mature cities had a weak CV reduction of 17.02%, indicating relatively weaker convergence. In contrast, growing cities displayed the highest level of CV in CEE, which had shown a fluctuating upward trend, with an average annual increase of 4.13%. There was no σ convergence observed for growing cities. These cities are in a rapid development phase where economic growth and improvements in CEE have not yet formed a virtuous cycle. The dependence on resource dividends and technological polarization has worsened the gap in CEE.

4.4.2. β convergence analysis

Before constructing the spatial convergence model, a two-tailed test of global spatial autocorrelation for CEE among

RBCs from 2006 to 2020 was conducted (**Table 5**). The results indicated that Moran's *I* index of CEE for RBCs showed a fluctuating upward trend, increasing from 0.062 in 2006 to 0.142 in 2020, suggesting a significant enhancement in spatial dependence. In terms of statistical significance, while the Moran's *I* values for 2007–2009 failed to pass the significance test, those for the remaining years were statistically significant. Moreover, since 2014, all values have reached significance at the 1% level. It showed that the spatial distribution of CEE among RBCs is not random; rather, it displayed a certain degree of spatial agglomeration. Analyzing the convergence of CEE in RBCs should consider geographic spatial factors, which can fully account for spatial correlation and heterogeneity.

Table 5. Global Moran's *I* index of CEE in RBCs from 2006 to 2020.

Year	Moran's *I*	Z value	P value
2006	0.062*	1.766	0.077
2007	0.046	1.315	0.189
2008	0.047	1.352	0.176
2009	0.057	1.610	0.107
2010	0.062*	1.712	0.087
2011	0.076**	2.051	0.040
2012	0.075**	2.014	0.044
2013	0.085**	2.247	0.025
2014	0.116***	2.966	0.003
2015	0.129***	3.281	0.001
2016	0.110***	2.845	0.004
2017	0.117***	3.006	0.003
2018	0.138***	3.514	0.000
2019	0.127***	3.243	0.001
2020	0.142***	3.610	0.000

*Note: *, **, and *** denote significance at the 10%, 5%, and 1% levels, respectively. The same applies hereinafter.*

Table 6. Spatial absolute *β* convergence results of CEE in RBCs from 2006 to 2020.

Variable	Overall	Growing	Mature	Declining	Regenerative
	SDM	SAR	SAR	SEM	SAR
Β	-0.312***	-0.289***	-0.262***	-0.445***	-0.220***
	(0.000)	(0.000)	(0.000)	(0.000)	(0.000)
ρ/λ	0.342***	0.300	0.188**	0.660***	0.853***
	(0.000)	(0.631)	(0.011)	(0.002)	(0.000)
Γ	0.217***				
	(0.002)				
V	0.0267	0.0244	0.0217	0.0421	0.0177
Year	Yes	Yes	Yes	Yes	Yes
City	Yes	Yes	Yes	Yes	Yes
R^2	0.050	0.055	0.056	0.090	0.059

Given that CEE varies across cities and may exhibit different spatial effects, this study adopted the methodology proposed by Elhorst (2010). We began by constructing a general panel regression model. We then employed the LM statistic to test for spatial autocorrelation to determine the most suitable model. If spatial autocorrelation is detected, we proceed with Wald and LR tests to decide which model is more appropriate. The results of the spatial absolute *β* convergence test for overall RBCs, along with the four subtypes, are presented in **Table 6**. The findings indicated: First, the overall RBCs and the four subtypes exhibited absolute *β* convergence, with all coefficients being significantly negative at the 1% confidence level. It suggested that, without considering exogenous factors affecting CEE, RBCs will converge to their respective steady-state levels over the long term. Second, the convergence speeds varied among RBCs. The overall convergence speed was 0.0267. Declining cities had a higher convergence speed with 0.0421, despite having a higher initial coefficient of variation (**Table 4**). The internal cities achieve a faster convergence rate through spatial synergy effects. In contrast, regenerative cities showed a slower convergence speed of 0.0177, likely due to the complex impacts of structural adjustments during the transition period, resulting in a relatively slower convergence process. Third, RBCs and the four subtypes exhibited different spatial effects. For the overall RBCs, both explanatory and dependent variables showed spatial lags, with ρ and γ being significantly positive at the 1% level. It indicated that the rate of change in CEE in one city is positively affected by the CEE and its rate of change in other cities. Growing, mature, and regenerative cities displayed spatial lags in the dependent variable while declining cities exhibited spatial error lags. It is important to note that the above analysis of absolute *β* convergence for overall RBCs and the four subtypes assumes similar levels of economic development, green technology progress, population density, environmental governance capacity, industrial structure advancement, and industrial structure rationalization. However, this assumption does not reflect reality. Therefore, further investigation into conditional *β* convergence is necessary to account for these regional differences.

Table 7 presents the results of the conditional *β* convergence test for CEE in overall RBCs and the four subtypes. The selection process of different spatial econometric models followed that used in the absolute *β* convergence analysis. The results showed the following. First, the overall RBCs and the four subtypes exhibited conditional *β* convergence. The convergence coefficients (*β*) were significantly negative at the 1% confidence level. It indicated that after accounting for factors such as economic development level, green technology progress, population density, environmental governance capacity, industrial structure advancement, and industrial structure rationalization, the CEE of these cities still tended to converge to their respective steady-state levels in the long run. Second, compared with absolute *β* convergence, the convergence speed for the overall RBCs, growing cities, and declining cities increased. However, it slowed down the convergence of mature and regenerative cities. Third, the overall group and the four subtypes of RBCs showed distinct spatial effects. Compared with the absolute *β* convergence analysis, only declining cities shifted from the Spatial Error Model (SEM) to the Spatial Durbin Model (SDM). However, the spatial autoregressive coefficient (*ρ*) and the spatial lag coefficient (*γ*) remained significantly positive at the 1% confidence level.

Table 7. Spatial conditional *β* convergence results of CEE in RBCs from 2006 to 2020.

Variable	Overall	Growing	Mature	Declining	Regenerative
	SDM	SAR	SAR	SDM	SAR
β	-0.314***	-0.297***	-0.260***	-0.457***	-0.211***
	(0.000)	(0.043)	(0.000)	(0.000)	(0.000)
ρ/λ	0.320***	0.300	0.181***	0.589***	0.838***
	(0.000)	(0.602)	(0.054)	(0.000)	(0.282)
GDP	-0.050	-0.189*	-0.098**	-0.070	0.026***
	(0.037)	(0.110)	(0.048)	(0.090)	(0.008)
GDP^2	0.004	0.010	0.007*	0.004	0.001
	(0.002)	(0.008)	(0.004)	(0.007)	(0.006)
GIP	0.240*	0.794*	0.084	0.556*	0.101
	(0.141)	(0.390)	(0.191)	(0.327)	(0.318)
POP	-0.002	0.002	-0.006**	0.006	-0.002
	(0.002)	(0.008)	(0.003)	(0.007)	(0.005)
ERL	0.231**	0.466*	0.397***	0.081	0.020
	(0.110)	(0.274)	(0.137)	(0.362)	(0.254)
ISA	0.017***	-0.011	0.006	0.048***	0.037***
	(0.005)	(0.016)	(0.007)	(0.016)	(0.013)
ISR	0.003	-0.100	0.027	0.021	0.098**
	(0.020)	(0.064)	(0.028)	(0.060)	(0.049)
Γ	0.206***			0.477***	
	(0.000)			(0.134)	
v	0.0269	0.0252	0.0215	0.0436	0.0169
Year	Yes	Yes	Yes	Yes	Yes
City	Yes	Yes	Yes	Yes	Yes
R^2	0.119	0.101	0.132	0.113	0.111

Additionally, after incorporating control variables into the conditional *β* convergence analysis, the R^2 values for all models, except for declining cities, showed a significant increase compared to the absolute *β* convergence analysis. It indicates that the selection of control variables is scientifically sound. From an economic perspective, there are notable differences in the influencing factors of CEE across different developmental stages of RBCs. Green technology progress, environmental governance capacity, and industrial structure advancement significantly positively impacted the CEE of overall RBCs, effectively promoting convergence towards higher values. However, economic development level, population density, and industrial structure rationalization did not significantly affect the rate of change in CEE. It does not imply that these factors lack influence on CEE; altering them can’t lead to a convergence towards lower or higher values of CEE.

From the perspective of control variables, mature cities exhibited an environmental Kuznets curve during their low-carbon development process. In the early stages of development, economic growth mainly relied on manufacturing and other high-energy-consuming, high-polluting industries, leading to increased carbon emissions as GDP grows. As cities further develop, technological advancements, industrial restructuring, and the implementation of environmental policies improved CEE. Green technological progress positively influenced the convergence of CEE in growing and declining cities. Improving environmental governance capacity led to enhanced CEE in both growing and mature cities.

Increased population density negatively impacted the convergence of CEE in mature cities. Industrial structure advancement positively affected declining and regenerative cities, while industrial structure rationalization significantly promoted the convergence of CEE in regenerating cities. Additionally, the spatial autoregressive coefficient (ρ) for overall RBCs and declining cities was significantly positive. The spatial error coefficient (λ) for mature and regenerating cities was also positive at the 1% confidence level. These coefficients played a crucial role in driving improvements in the CEE of neighboring regions.

5. Conclusions and policy implications

This study selected 110 RBCs in China from 2006 to 2020 as the research sample. The study utilized the super EBM-DEA model to assess CEE, analyzing its spatiotemporal evolution characteristics and features of the spatial correlation network. From a combined perspective of absolute and relative differences, the study clarified the regional differences in CEE of RBCs and its sources at the overall and subtypes. Furthermore, convergence analysis was carried out through σ convergence, spatial absolute β convergence, and spatial conditional β convergence to explore the convergence or divergence trends. The main findings are as follows. (1) The CEE in the overall RBCs and four subtypes showed a fluctuating upward trend, with the general pattern presenting as “regenerating > growing > mature > declining.” (2) In terms of spatial correlation network characteristics, the CEE among RBCs exhibited a complex structure involving multiple nodes and multi-threaded linkages, with geographically adjacent connections and inter-regional interactions coexisting. Inter-regional linkage was the dominant form of association. Meanwhile, the core cities within the network had transitioned from traditional industrial centers in central and western China to a more diverse set of city types. (3) Regarding regional differences, the absolute differences in CEE across all RBCs generally declined over time. Among the four subtypes, the trends in absolute differences for mature, declining, and regenerating cities were consistent with the overall trend, while growing cities displayed signs of internal multi-polarity. The relative differences in CEE across all RBCs continued to narrow, with transvariation density identified as the primary contributor to these differences. Among the four types of cities, only growing cities exhibited an “M”-shaped growth trend in intra-type relative differences. (4) The CEE of the overall RBCs and mature, declining, and regenerating cities demonstrated characteristics of σ convergence, spatial absolute β convergence, and spatial conditional β convergence. Growing cities, however, did not exhibit σ convergence, although they still showed evidence of spatial absolute β convergence and spatial conditional β convergence. Different types of cities also displayed distinct spatial effects. Moreover, the impacts of factors such as economic development level, green technology progress, and industrial structure on the convergence of CEE varied across cities, indicating heterogeneity in the driving forces behind efficiency improvements.

Improving CEE is crucial for the green transformation and sustainable development of RBCs. It is also an inevitable choice for China to achieve its “carbon peak and carbon neutrality” goals. In light of this, the study proposes the following policy implications. Firstly, the Chinese government should still pay attention to the green transformation of RBCs and continuously promote the detailed implementation of sustainable development policies. Each region must adhere to the overall guidance of green and high-quality development, gradually shifting towards a development model dominated by clean industries. Urban development must not only achieve low-carbon status in existing industries but also focus on the low-carbon nature of new developments. The relevant government departments should strictly control the qualifications and procedures for urban resource exploitation, effectively reducing negative impacts on the ecological environment.

Secondly, in line with spatial correlation network characteristics of RBCs, making efforts to promote cross-regional cooperation. Facilitating exchanges and collaborations among different types of cities in low-carbon technologies and resource management can fully leverage the exemplary role of mature and regenerating cities. Given that declining cities have weaker internal regional connections, the Chinese government needs to increase policy support, providing financial and technical assistance to vigorously support the development of replacement industries, gradually enhancing their sustainable development capabilities. Establishing several national-level low-carbon technology transfer centers could form a cooperative and mutual assistance mechanism across all RBCs, optimizing the spatial correlation network of CEE and fully leveraging the positive externalities of such networks.

Thirdly, pay attention to the balance of emission reduction and decarbonization efforts in RBCs. Growing cities exhibit significant internal regional differences in CEE, which are related to varying levels of urban development. Growing cities are in an upward phase of resource exploitation and substantial resource security potential. Intra-regional cities should develop differentiated policies based on their developmental stages and resource endowments. Supporting high-emission cities in accelerating green transformation and encouraging cities with better foundations to lead by example can establish a collaborative development mechanism where core cities drive the surrounding smaller cities, promoting industrial division and resource sharing, thereby narrowing internal regional development disparities.

Lastly, considering the socio-economic factors driving the convergence of CEE in RBCs, tailored emission reduction and decarbonization policies should be developed according to local conditions. Efforts should focus on fostering a green economy, fully unleashing the vitality of scientific and technological innovation. The government should tackle hard technology, optimize industrial layouts, adjust industrial structures, and improve environmental governance capabilities. Leveraging the benefits of digital dividends, strengthening talent team building in the new era, and promoting breakthroughs in urban green transformation should be prioritized.

Competing interests

The authors declare that they have no known competing financial interests or personal relationships that could have appeared to influence the work reported in this study.

Author Contributions

Wenjing Bao: Conceptualization, Methodology, Software, Visualization, Formal analysis, Data curation, Writing-original draft. **Haifeng Xiao:** Supervision, Writing-review & editing, Funding acquisition.

Data availability

Data are available from the author on reasonable request.

Funding

This study was supported by the Ministry of Agriculture and Rural Affairs and the Ministry of Finance Project of the People's Republic of China (CARS-39-22).

References

Andersen, P. and Petersen, N.C. (1993) A Procedure for Ranking Efficient Units in Data Envelopment Analysis, Management Science, 39(10), 1261–1264.

Bai, R. and Lin, B. (2024) An in-depth analysis of green innovation efficiency: New evidence based on club convergence and spatial correlation network, Energy Economics, 132, 107424.

Baloch, Z.A., Tan, Q., Iqbal, N., Mohsin, M., Abbas, Q., Iqbal, W. and Chaudhry, I.S. (2020) Trilemma assessment of energy intensity, efficiency, and environmental index: evidence from BRICS countries, Environmental Science and Pollution Research, 27(27), 34337–34347.

Balsalobre-Lorente, D., Bekun, F.V., Etokakpan, M.U. and Driha, O.M. (2019) A road to enhancements in natural gas use in Iran: A multivariate modelling approach, Resources Policy, 64, 101485.

Chen, H., Yi, J., Chen, A., Peng, D. and Yang, J. (2023) Green technology innovation and CO2 emission in China: Evidence from a spatial-temporal analysis and a nonlinear spatial durbin model, Energy Policy, 172, 113338.

Chen, P. (2024) The spatial impacts of the circular economy on carbon intensity-new evidence from the super-efficient SBM-DEA model, Energy & Environment, 35(1), 47–63.

Cui, L., Chen, L. and Yang, X. (2024) Evaluation and analysis of green efficiency of China’s coastal ports under the ‘double carbon’ goal: two improved DEA models with CO2 emissions, Environment, Development and Sustainability, 26(11), 29099–29128.

Dagum, C. (1997) A new approach to the decomposition of the Gini income inequality ratio, Empirical Economics, 22(4), 515–531.

Dong, F., Yu, B., Hadachin, T., Dai, Y., Wang, Y., Zhang, S. and Long, R. (2018) Drivers of carbon emission intensity change in China, Resources, Conservation and Recycling, 129, 187–201.

Dong, H., Zhang, P., Dong, H. and Jia, N. (2025) The spatiotemporal dynamic evolution characteristics of carbon emissions in less developed resource-based cities: evidence from Pingliang City, China, Scientific Reports, 15(1), 11266.

Duman, Z., Mao, X., Cai, B., Zhang, Q., Chen, Y., Gao, Y. and Guo, Z. (2023) Exploring the spatiotemporal pattern evolution of carbon emissions and air pollution in Chinese cities, Journal of Environmental Management, 345, 118870.

Elhorst, J.P. (2010) Applied Spatial Econometrics: Raising the Bar, Spatial Economic Analysis, 5(1), 9–28.

Färe, R., Grosskopf, S. and Pasurka, C.A. (2007) Environmental production functions and environmental directional distance functions, Energy, 32(7), 1055–1066.

Gao, P., Yue, S. and Chen, H. (2021) Carbon emission efficiency of China’s industry sectors: From the perspective of embodied carbon emissions, Journal of Cleaner Production, 283, 124655.

Gao, Y. and Gao, M. (2024) Spatial correlation network of municipal solid waste carbon emissions and its influencing factors in China, Environmental Impact Assessment Review, 106, 107490.

Gao, Y., Gao, X. and Zhang, X. (2017) The 2 °C Global Temperature Target and the Evolution of the Long-Term Goal of Addressing Climate Change—From the United Nations Framework Convention on Climate Change to the Paris Agreement, Engineering, 3(2), 272–278.

Goldsmith, R.W. (1951) A Perpetual Inventory of National Wealth, in Studies in Income and Wealth, Volume 14. National Bureau of Economic Research, Inc, 5–73.

Gong, Q. (2024) Green transformation paths of resource-based cities in China from the configuration perspective, Regional Sustainability, 5(3), 100158.

Guo, C. and Yu, J. (2024) Determinants and their spatial heterogeneity of carbon emissions in resource-based cities, China, Scientific Reports, 14(1), 5894.

Han, X., Yu, J., Xia, Y. and Wang, J. (2021) Spatiotemporal characteristics of carbon emissions in energy-enriched areas and the evolution of regional types, Energy Reports, 7, 7224–7237.

Heidenreich, N.-B., Schindler, A. and Sperlich, S. (2013) Bandwidth selection for kernel density estimation: a review of fully automatic selectors, AStA Advances in Statistical Analysis, 97(4), 403–433.

Hou, J., Shi, C., Fan, G. and Xu, H. (2024) Research on the impact and intermediary effect of carbon emission trading policy on carbon emission efficiency in China, Atmospheric Pollution Research, 15(4), 102045.

Huang, H. and Yi, M. (2023) Impacts and mechanisms of heterogeneous environmental regulations on carbon emissions: An empirical research based on DID method, Environmental Impact Assessment Review, 99, 107039.

Jiang, Y., Qiao, S., Chen, S., Ying, R., and Zhang, Y. (2024) Environmental regulation, hog scale production and the synergy of pollution control and carbon reduction, Global NEST Journal, 26(4), 05696.

Khalid, K., Hussain, B. and Ali, S. (2021) Evaluating eco-efficiency in consumption and production through sustainable utilization of resources: A panel analysis of APAC by population, Renewable Energy, 170, 1096–1106.

Li, K., Zhou, Y., Huang, X., Xiao, H. and Shan, Y. (2024) Low-carbon development pathways for resource-based cities in

China under the carbon peaking and carbon neutrality goals, Environmental Science and Pollution Research, 31(7), 10213–10233.

Li, L., Shan, Y., Lei, Y., Wu, S., Yu, X., Lin, X. and Chen, Y. (2019) Decoupling of economic growth and emissions in China’s cities: A case study of the Central Plains urban agglomeration, Applied Energy, 244, 36–45.

Li, M., Xiao, H. and Pan, Z. (2024) Spatial correlation network structure of carbon productivity from the livestock sector in China and its driving factors: a perspective of social network analysis, Global NEST Journal, 26(6), 06125.

Liao, Q., Li, P., Bin Roosli, R., Liu, S., Zhang, X., Zhang, C., Wang, Y., Wu, L. and Yao, H. (2022) Carbon Emission Characteristics of Resource-Based Cities in China, Iranian Journal of Science and Technology-Transactions of Civil Engineering, 46(6), 4579–4591.

Liu, C., Xie, R. and Ma, C. (2025) Convergence of Chinese urban carbon marginal abatement cost, Applied Economics, 57(5), 525–542.

Lu, P., Li, Z., Wen, Y., Liu, J., Yuan, Y., Niu, R., Wang, Y. and Han, L. (2023) Fresh insights for sustainable development: Collaborative governance of carbon emissions based on social network analysis, Sustainable Development, 31(3), 1873–1887.

Murshed, M., Apergis, N., Alam, M.S., Khan, U. and Mahmud, S. (2022) The impacts of renewable energy, financial inclusivity, globalization, economic growth, and urbanization on carbon productivity: Evidence from net moderation and mediation effects of energy efficiency gains, Renewable Energy, 196, 824–838.

Niu, J., Jin, G. and Zhang, L. (2023) Territorial spatial zoning based on suitability evaluation and its impact on ecosystem services in Ezhou city, Journal of Geographical Sciences, 33(11), 2278–2294.

Qiu, F., Yuan, H., Bai, L. and Li, F. (2017) Spatial-temporal heterogeneity of industrial structure transformation and carbon emission effect in Xuzhou Metropolitan Area, Chinese Geographical Science, 27(6), 904–917.

Qu, X. and Lee, L. (2015) Estimating a spatial autoregressive model with an endogenous spatial weight matrix, Journal of Econometrics, 184(2), 209–232.

Shan, Y., Guan, Y., Hang, Y., Zheng, H., Li, Y., Guan, D., Li, J., Zhou, Y., Li, L. and Hubacek, K. (2022) City-level emission peak and drivers in China, Science Bulletin, 67(18), 1910–1920.

Shen, N., Peng, H. and Wang, Q. (2021) Spatial dependence, agglomeration externalities and the convergence of carbon productivity, Socio-Economic Planning Sciences, 78, 101060.

Solow, R. (1988) Growth Theory and After, American Economic Review, 78(3), 307–317.

Song, W., Yin, S., Zhang, Y., Qi, L. and Yi, X. (2022) Spatial-temporal evolution characteristics and drivers of carbon emission intensity of resource-based cities in China, Frontiers in Environmental Science, 10, 972563.

Su, Y. and Xu, G. (2025) The Influencing Mechanism of Intelligent Production on Carbon Emission Efficiency of Equipment Manufacturing Industry in China, Processes, 13(4), 1102.

Tan, F., Yang, S. and Niu, Z. (2023) The impact of urbanization on carbon emissions: both from heterogeneity and mechanism test, Environment, Development and Sustainability, 25(6), 4813–4829.

Tone, K. and Tsutsui, M. (2010) An epsilon-based measure of efficiency in DEA – A third pole of technical efficiency, European Journal of Operational Research, 207(3), 1554–1563.

Wang, G., Deng, X., Wang, J., Zhang, F. and Liang, S. (2019) Carbon emission efficiency in China: A spatial panel data analysis, China Economic Review, 56, 101313.

Wang, S., Gao, S., Huang, Y. and Shi, C. (2020) Spatiotemporal evolution of urban carbon emission performance in China and prediction of future trends, Journal of Geographical Sciences, 30(5), 757–774.

Wang, Y. and Zheng, Y. (2021) Spatial effects of carbon emission intensity and regional development in China, Environmental Science and Pollution Research, 28(11), 14131–14143.

Wu, C., Deng, H., Zhao, H. and Xia, Q. (2025) Spatiotemporal evolution and convergence patterns of urban carbon emission efficiency in China, Humanities & Social Sciences Communications, 12(1), 675.

Xiao, Y., Ma, D., Zhang, F., Zhao, N., Wang, L., Guo, Z., Zhang, J., An, B. and Xiao, Y. (2023) Spatiotemporal differentiation of carbon emission efficiency and influencing factors: From the perspective of 136 countries, Science of The Total Environment, 879, 163032.

Xiang, S., Huang, X., Lin, N. and Yi, Z. (2025) Synergistic reduction of air pollutants and carbon emissions in Chengdu-Chongqing urban agglomeration, China: Spatial-temporal characteristics, regional differences, and dynamic evolution, Journal of Cleaner Production, 493, 144929.

Xie, P., Guo, W., Lin, X., Shu, Y., Sun, F. and Huang, B. (2025) Study on the measurement of interprovincial carbon emission performance, regional gaps, and spatial convergence in China, Energy, 317, 134597.

Xing, P., Wang, Y., Ye, T., Sun, Y., Li, Q., Li, X., Li, M. and Chen, W. (2024) Carbon emission efficiency of 284 cities in China based on machine learning approach: Driving factors and regional heterogeneity, Energy Economics, 129, 107222.

Xu, C., Xu, Y., Chen, J., Huang, S., Zhou, B. and Song, M. (2023) Spatio-temporal efficiency of fiscal environmental expenditure in reducing CO2 emissions in China’s cities, Journal of Environmental Management, 334, 117479.

Xue, L., Zheng, Z., Meng, S., Li, M., Li, H. and Chen, J. (2022) Carbon emission efficiency and spatio-temporal dynamic evolution of the cities in Beijing-Tianjin-Hebei Region, China, Environment, Development and Sustainability, 24(6), 7640–7664.

Yu, Y. and Zhang, N. (2021) Low-carbon city pilot and carbon emission efficiency: Quasi-experimental evidence from China, Energy Economics, 96, 105125.

Zeng, G., Sang, Y., Gui, Q., Li, J., Yuan, J. and Zhu, K. (2024) Research on carbon emission efficiency and spatial-temporal factors in the transportation industry: Evidence from the Yangtze river economic belt, Global NEST Journal, 26(4), 05638.

Zhang, C. and Chen, P. (2021) Industrialization, urbanization, and carbon emission efficiency of Yangtze River Economic Belt—empirical analysis based on stochastic frontier model, Environmental Science and Pollution Research, 28(47), 66914–66929.

Zheng, H., Wu, Y., He, H., Delang, C.O., Lu, J., Yao, Z. and Dong, S. (2024) Urbanization and urban energy eco-efficiency: A meta-frontier super EBM analysis based on 271 cities of China, Sustainable Cities and Society, 101, 105089.

Zheng, W., Kan, Z., Jie, F. and Hao, Z. (2023) Progress of research on energy-related carbon emission accounting methods at the prefectural and county levels, Progress in Geography, 42(7), 1406–1419.